Original research paper

An Analysis of Axial Couette Flow in Annular Region of Abruptly Stopped Pipes

ABSTRACT

Aims: Flow in annular regions encounters in many fields such as bio-medical, petroleum, aerospace and chemical industries and among them, the flow between two coaxial pipes has rather become interesting due to its asymmetry nature.
Study design: Theoretical solution and numerical approximation and analysis.
Place and Duration of Study: Department of mathematics, Faculty of Science, University of Peradeniya, Sri Lanka, between August 2017 and January 2018.
Methodology: Yet it is particularly challenging to obtain theoretical solutions. In this paper, we carried out a comprehensive analysis for unsteady, unidirectional and incompressible Couette flow between annulus, when inner and outer pipes were brought to abrupt stop from constant velocities. The velocity of the field is derived by applying the Laplace transformation method. The analytical work is supported by the numerical approximation using Finite Difference Method, which was implemented in MATLAB programming. We illustrate results varying radii of the outer and inner pipe captured by ratio ($\eta = 0.1, 0.3, 0.5 \; and \; 0.7$) and for different boundary conditions. Flow field was visualized using FDM approximation for selected parameter regime when the flow was suddenly stopped.
Results: Asymmetry of the velocity profile was affected by different radius ratios ($\eta = 0.1, 0.3, 0.5 \; and \; 0.7$). Unsteadiness in the flow field was happened due to sudden changes in flow parameters.
Conclusion: The results depicted that radii ratio and boundary condition has a strong impact on the role on changing the flow characteristics and flow parameters.

Keywords: Couette flow, Asymmetry velocity, Navier-Stokes equations, Radii ratios

1. INTRODUCTION

The study of flow through an annulus bounded by two coaxial pipes has attracted the attention of researches due to its peculiarity nature and the flow geometry is one which has found considerable practical application in the process industries. The concentric annulus also presents a flow system which is still amenable to analysis. Nevertheless, in this seemingly simple flow field some rather strange and puzzling phenomena occur. The most interesting of these are associated with the transition from laminar to non-laminar [1].
The unsteady laminar Couette flow in concentric annulus, where the geometry is shown in , is investigated to predict the surge or swab pressure encountered when running or pulling pipes in a liquid-filled borehole. The motion equations were analytically solved in [2] for power-law fluids by the perturbation method. During the drilling operation of oil and gas wells, the velocity field varies along the well length and the resulting flow model is three-dimensional. Lubrication theory has been used to simplify the governing equations into a two dimensional differential equation that describes the pressure field and velocity in each cross section was analysed for different cases in [3]. In [4], stability and transition to turbulence of wall-bounded unsteady velocity profiles with reverse flow was investigated. Experiment and theoretical investigations of instability and evolution of reverse flow that occurred in a decelerating flow has been performed where the flow is generated by the controlled piston motion. The procedure to obtain analytical solution for unsteady laminar flow in an infinitely long pipe with circular cross section and in an infinitely long two dimensional channel, created by an arbitrary but given volume flow rate with time was presented in [5].

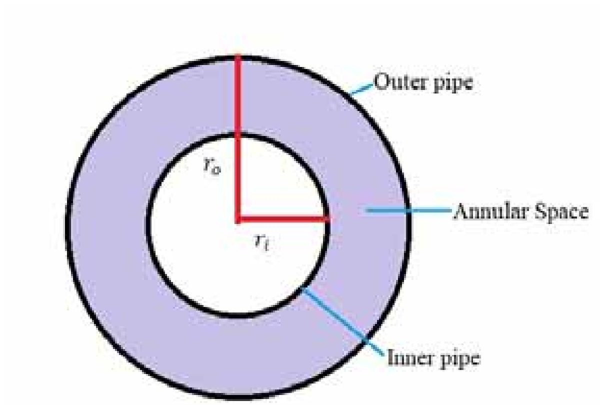

Fig. 1. Schematic description of annular space bounded by concentric pipes (radius of the inner pipe: r_i and radius of the outer pipe: r_o)

Some properties of the time dependent Navier-Stokes equation for impulsively started from rest by sudden application of a constant pressure gradient or by the impulsive motion of a boundary was discussed in [6] and a satellite reaction control subsystem was explained in [7]. A flow channel network numerical scheme is used to determine the blow down pressure profile and the steady state pressure drops in the propellant lines. This study give the idea about damaged to the propulsion components or lines due to the sudden closure of fuel valves.
Moreover, an analytical solution to the flow through the pipe and the annular space between two concentric pipes has been obtained for the case of one-dimensional unsteady flow in [8]. However, the solution obtained were only when the volume flow rate is provided. Analytical solution of the unsteady laminar bi-directional flow between concentric pipes with known volume flow rate has been derived for various cases in [9]. A new analytical solution for unsteady bi-directional flow through an annulus between two concentric pipes with a prescribed time dependent volume flow rate has also been obtained in [10]. Analytically obtained velocity profiles are compared with experimental data and also numerical results [11] and they are used for determining the linear stability characteristics of such flows. Yet, the analysis when annular boundaries have abrupt changes is still scarce.
In the present work, we carry out an analysis of suddenly stopped Couette flow. Initially the flow was considered as independent of time and subsequently, the pipes were brought to abrupt rest and the flow then depends on time. This sudden change in boundaries encounters in many industrial processes. Asymmetry, radii ratio and unsteadiness of the annular flow have significant but different role in flow instability and transition.
The paper is organized as follows. In section 2, the unsteady and incompressible flow in a concentric annulus for abruptly stopped axial Couette flow is investigated. Exact analytical solution methodology for incompressible, unidirectional and unsteady flow is presented. In section 3, Finite Difference Method is discussed to approximate the flow characteristics in the annular region and the approximate values for axial Couette flow for various cases are presented. In section 5, the present work and the scope for future work were summarized.

2. METHODOLOGY

2.1 Theoretical Implementation

An annular region between a long inner pipe of radius, r_i^* and a coaxial outer pipe of radius, r_0^* is considered in the study. The flow is taken to be at steady state in the annular region, before making the abrupt changes to the boundary. Cylindrical co-ordinates system (r^*, θ, x^*) is employed due and, r^*, θ, and x^* indicates the radial, azimuthal and axial directional co-ordinates respectively. Corresponding velocity components in axial, radial and azimuthal directions are defined as v_r^*, v_θ^* and v_x^* respectively. The superscript "*" is used to denote dimensional quantities. The simplified Navier-Stokes equation was written as when the flow was assumed to be axisymmetric, incompressible, unidirectional, fully developed, entirely depend on the wall movement (no-slip boundary condition) and has no body force. Hence, simplified Navier-Stokes equations for steady and unsteady flow are as below in equations (1) and (2) respectively.

$$\frac{1}{r^*}\frac{\partial}{\partial r^*}\left(r^*\frac{\partial v_x^*}{\partial r^*}\right) = 0 \tag{1}$$

$$\rho\left(\frac{\partial v_x^*}{\partial t^*}\right) = \mu\left[\frac{1}{r^*}\frac{\partial}{\partial r^*}\left(r^*\frac{\partial v_x^*}{\partial r^*}\right)\right] \tag{2}$$

Dimensionless parameters introduced with special co-ordinates are normalized by Re (Reynolds number), while velocity and time are made dimensionless by U_c and $\frac{U_c}{R_c}$, respectively; where, R_c and U_c were characteristic length and velocity respectively. Thus, the non-dimensional variables and parameters are written as,

$$v_x = \frac{v^*{}_x}{U_c}; \quad r = \frac{r^*}{R_c}; \quad t = \frac{t^* U_c}{R_c}; \quad Re = \frac{U_c R_c \rho}{\mu} \tag{3}$$

2.1.1 Steady State Solution

$$v_x(r,0) = C_1 + C_2 \ln(r) \tag{4}$$

$$v_x(r_i\,,t) = V_i; \quad v_x(r_o\,,t) = V_o \tag{5}$$

Equations (4) and (5) were dimensionless initial and inner and outer boundary conditions respectively for steady governing equation. Where, initial condition was obtained from the literature study in [12] and boundary conditions were assumed as constant velocities.

Hence, the solution for the steady state equation can be written as,

$$v_x(r\,,t) = \frac{V_o - V_i}{2} + \frac{V_i - V_o}{2ln(\eta)}\left[2ln(r) - ln(r_o r_i)\right] \tag{6}$$

Let,

$$D_1 = \frac{V_o + V_i}{2}; \quad D_2 = \frac{V_i - V_o}{2ln(\eta)}\, ln(r_o r_i); \quad D_3 = \frac{V_i - V_o}{ln(\eta)} \tag{7}$$

And, $D_{12} = D_1 - D_2$. Thus, the simplified steady state solution is written as,

$$v_x = D_{12} + D_3\, ln(r) \tag{8}$$

2.1.2 Unsteady Solution

$$v_x(r,0) = D_{12} + D_3\, ln(r) \tag{9}$$

$$v_x(r_i\,,t) = F_i; \quad v_x(r_o\,,t) = F_o \tag{10}$$

The equations (9) and (10) are dimensionless initial and inner and outer boundary conditions respectively for unsteady governing equation. Initial condition for the unsteady equation is the solution of the steady state equation.

Laplace transforms of dimensionless unsteady equation and boundary conditions are,

$$\frac{d^2\bar{v}_x(r,s)}{dr^2} + \frac{1}{r}\frac{d\bar{v}_x(r,s)}{dr} - Re\; s\; \bar{v}_x(r,s) = -Re\; v_x(r,0) \tag{11}$$

$$\bar{v}_x(r_i\,,s) = \bar{F}_i; \quad \bar{v}_x(r_o\,,s) = \bar{F}_o \tag{12}$$

Here, the over bar quantities were transformed variables. Hence, $v_x(r,0) = D_{12} + D_3\, ln(r)$ is due to the choice of initial condition. The equation (11) is a second order, non-homogeneous and ordinary differential equation. Since the governing equation and boundary conditions are known, the problem was well posed.

$$\frac{d^2\bar{v}_x(r,s)}{dr^2} + \frac{1}{r}\frac{d\bar{v}_x(r,s)}{dr} - Re\; s\; \bar{v}_x(r,s) = -Re\left[D_{12} + D_3\, ln(r)\right] \tag{13}$$

Here, $Re\, s = q^2$. In the equation (13), the homogeneous part is the modified Bessel equation of highest order [13,14]. Homogeneous and non-homogeneous solutions are,

$$\bar{v}_{x_{homogeneous}} = \phi_1 \mathrm{I}_0(qr) + \phi_2 \mathrm{K}_0(qr) \tag{14}$$

$$\bar{v}_{x_{non-homogeneous}} = -\left[D_{12} + D_3\, ln(r)\right] \tag{15}$$

Thus, the complete solution is,

$$\bar{v}_x = \phi_1 \mathrm{I}_0(qr) + \phi_2 \mathrm{K}_0(qr) - \left[D_{12} + D_3\, ln(r)\right] \tag{16}$$

Here, I_0 and K_0 are highest order modified Bessel functions of first and second kind respectively. ϕ_1 and ϕ_2 were the arbitrary constants, determined by using boundary conditions (10) in equation (16).

To find the non-homogeneous solution, Wronskian [15] is given as,

$$W\left[\mathrm{I}_0(qr), \mathrm{K}_0(qr)\,\right] = \begin{vmatrix} \mathrm{I}_0(qr) & \mathrm{K}_0(qr) \\ \mathrm{I}_0'(qr) & \mathrm{K}_0'(qr) \end{vmatrix} = -\frac{1}{r} \tag{17}$$

$$\bar{v}_{x1_{non-homogeneous}} = -\mathrm{I}_0(qr)\int \frac{\begin{Bmatrix} \mathrm{K}_0(qr) \\ [-Re\, D_3\, ln(r)] \end{Bmatrix}}{-\frac{1}{r}} dr + \mathrm{K}_0(qr)\int \frac{\begin{Bmatrix} \mathrm{I}_0(qr) \\ [-Re\, D_3\, ln(r)] \end{Bmatrix}}{-\frac{1}{r}} dr \quad (18)$$

$$\bar{v}_{x2_{non-homogeneous}} = -\mathrm{I}_0(qr)\int \frac{\begin{Bmatrix} \mathrm{K}_0(qr) \\ [-Re\, D_{12}] \end{Bmatrix}}{-\frac{1}{r}} dr + \mathrm{K}_0(qr)\int \frac{\begin{Bmatrix} \mathrm{I}_0(qr) \\ [-Re\, D_{12}] \end{Bmatrix}}{-\frac{1}{r}} dr \quad (19)$$

Thus, the non-homogeneous solution is written as,

$$\bar{v}_{x_{non-homogeneous}} = \bar{v}_{x1_{non-homogeneous}} + \bar{v}_{x2_{non-homogeneous}} \quad (20)$$

From equation (16), the solution in transformed domain is written as,

$$\bar{v}_x = \phi_1 \mathrm{I}_0(qr) + \phi_2 \mathrm{K}_0(qr) + \frac{D_{12}}{s} + \frac{D_3\, ln(r)}{s} \quad (21)$$

Applying the boundary conditions (12) in the equation (21), we can find the arbitrary constants ϕ_1 and ϕ_2. Then the equation (21) was written as,

$$\bar{v}_x = \left\{ \frac{\begin{Bmatrix} \left[\bar{F}_i - \frac{D_{12}}{s} - \frac{D_3}{s} ln(r_i)\right] [\mathrm{I}_0(qr_o)\mathrm{K}_0(qr) - \mathrm{K}_0(qr_o)\mathrm{I}_0(qr)] \\ + \left[\bar{F}_o - \frac{D_{12}}{s} - \frac{D_3}{s} ln(r_o)\right] [\mathrm{K}_0(qr_i)\mathrm{I}_0(qr) - \mathrm{I}_0(qr_i)\mathrm{K}_0(qr)] \end{Bmatrix}}{\mathrm{K}_0(qr_i)\mathrm{I}_0(qr_o) - \mathrm{I}_0(qr_i)\mathrm{K}_0(qr_o)} \right\} + \left[\frac{D_{12} + D_3\, ln(r)}{s}\right] \quad (22)$$

If the boundary conditions are constants, then $\bar{F}_i = \frac{F_i}{s}$ and $\bar{F}_o = \frac{F_o}{s}$.

$$qr_i = r_i\sqrt{Re}\sqrt{s} = A\sqrt{s}; \quad qr_o = r_0\sqrt{Re}\sqrt{s} = B\sqrt{s}; \quad qr = r\sqrt{Re}\sqrt{s} = C\sqrt{s} \quad (23)$$

Here, $= r_i\sqrt{Re}$; $B = r_0\sqrt{Re}$ and $C = r\sqrt{Re}$.

The flow velocity is,

$$\bar{v}_x = \left\{ \frac{\begin{Bmatrix} \left[\bar{F}_i - \frac{D_{12}}{s} - \frac{D_3}{s} ln(r_i)\right] \\ \left[\mathrm{I}_0(B\sqrt{s})\mathrm{K}_0(C\sqrt{s}) - \mathrm{K}_0(B\sqrt{s})\mathrm{I}_0(C\sqrt{s})\right] \\ + \left[\bar{F}_o - \frac{D_{12}}{s} - \frac{D_3}{s} ln(r_o)\right] \\ \left[\mathrm{K}_0(A\sqrt{s})\mathrm{I}_0(C\sqrt{s}) - \mathrm{I}_0(A\sqrt{s})\mathrm{K}_0(C\sqrt{s})\right] \end{Bmatrix}}{s\left[\mathrm{K}_0(A\sqrt{s})\mathrm{I}_0(B\sqrt{s}) - \mathrm{I}_0(A\sqrt{s})\mathrm{K}_0(B\sqrt{s})\right]} \right\} + \left[\frac{D_{12} + D_3\, ln(r)}{s}\right] \quad (24)$$

Moreover, the solution in time domain $v_x(r,t)$ was obtain by taking the inverse Laplace transform of $\bar{v}_x(r\,,s)$. The inverse transform of equation (24) can be obtained using the convolution theorem. Applying convolution theorem to equation (24), we can obtain,

$$v_x(r\,,t) = \frac{1}{2\pi i}\int_{r-i\infty}^{r+i\infty} \bar{v}_x(r\,,s)\; exp\,(r,s)\, dt \quad (25)$$

We can write the integrand in the form of $\frac{a\Gamma^{n+1}}{b\Gamma^n}$, where, Γ is the radius of the Bromwich contour taken; such that all the poles lie in the left of the contour. The integrand diverges as $\Gamma \to \infty$, preventing the application of the convolution theorem, Hence, we take the inverse Laplace transform [16] of equation (24) and obtain the solution in time domain.

$$v_x(r\,,t) = \sum \left\{ \begin{matrix} residue\ of\ poles\ of \\ [\bar{v}_x(r\,,s) exp\,(r,s)] \end{matrix} \right\} \tag{26}$$

Thus, the complete final solution was written as,

$$v_{x_1} = \left\{ \frac{\pi r_o^2 Re[F_i - D_{12} - D_3 ln(r_i)] \begin{bmatrix} \mathrm{Y}_0(a_n)\mathrm{J}_0\left(\frac{C}{B}a_n\right) \\ -\mathrm{J}_0(a_n)\mathrm{Y}_0\left(\frac{C}{B}a_n\right) \end{bmatrix} exp\left(-\frac{a_n^2 t}{r_o^2 Re}\right)}{2a_n^2\left(\frac{dD}{dS}\right)_{s=-\frac{a_n^2}{B^2}}} \right\} \tag{27}$$

$$+\frac{ln\frac{r}{r_o}}{ln\frac{A}{B}}\left[\bar{F}_i - \frac{D_{12}}{s} - \frac{D_3}{s} ln(r_i)\right]$$

$$v_{x_2} = \left\{ \frac{\pi r_o^2 Re[F_o - D_{12} - D_3 ln(r_o)] \begin{bmatrix} \mathrm{J}_0\left(\frac{A}{B}a_n\right)\mathrm{Y}_0\left(\frac{C}{B}a_n\right) \\ -\mathrm{Y}_0\left(\frac{A}{B}a_n\right)\mathrm{J}_0\left(\frac{C}{B}a_n\right) \end{bmatrix} exp\left(-\frac{a_n^2 t}{r_o^2 Re}\right)}{2a_n^2\left(\frac{dD}{dS}\right)_{s=-\frac{a_n^2}{B^2}}} \right\} \tag{28}$$

and

$$v_{x_3} = D_{12} + D_3\, ln(r) \tag{29}$$

Thus, the velocity in time domain:

$$v_x(r\,,t) = v_{x_1} + v_{x_2} + v_{x_3} \tag{30}$$

When F_i and F_o are assumed to be zero in the equation (30), the exact analytical solution is obtained for the abruptly stopped axial Couette flow. Note that, since the flow was entirely depend on the wall movement, the pressure difference throughout the annulus in axial direction was not considered. A numerical implementation was carried out to visualize the flow field for different ratios.

2.2 Numerical Implementation

The numerical implementation, starts with the non-dimensional form of equation (2), where the dependent variable, v_x (velocity in axial direction) and the independent variables, r (radius between inner and outer pipes) and t (time). To approximate the solution of the unsteady equation using Finite Difference method, solution of the steady state equation was taken as initial condition (9). Using central space difference approximation the second order partial derivative with respect to radius and the first order partial derivative with respect to radius of the equations are approximated as,

$$v_x''(r) \simeq \left\{ \frac{\begin{bmatrix} U(r-\Delta r) - 2\,U(r) \\ +\,U(r+\Delta r) \end{bmatrix}}{(\Delta r)^2} \right\} + O(\Delta r)^2 \tag{31}$$

$$v_x'(r) \simeq \left[\frac{U(r+\Delta r) - U(r-\Delta r)}{2\Delta r}\right] + O(\Delta r)^2 \tag{32}$$

Using the forward time difference approximation the first order partial derivative with respect to time is approximated as,

$$v_x'(t) \simeq \left[\frac{U(t+\Delta t) - U(t)}{\Delta t}\right] + O(\Delta t)^2 \tag{33}$$

Thus, the discretized equation with $\Delta t = k$ and $\Delta r = h$ is as,

$$\frac{v_{x_{i,j+1}} - v_{x_{i,j}}}{k} = \frac{1}{Re}\left\{ \begin{matrix} \left[\frac{\begin{pmatrix} v_{x_{i+1,j}} - 2\,v_{x_{i,j}} \\ +\,v_{x_{i-1,j}} \end{pmatrix}}{h^2}\right] \\ +\frac{1}{r}\left[\frac{v_{x_{i+1,j}} - v_{x_{i-1,j}}}{2h}\right] \end{matrix} \right\} \tag{34}$$

Here, $i = 0,1,2,3, \ldots, M$ and $j = 0,1,2,3, \ldots, N$

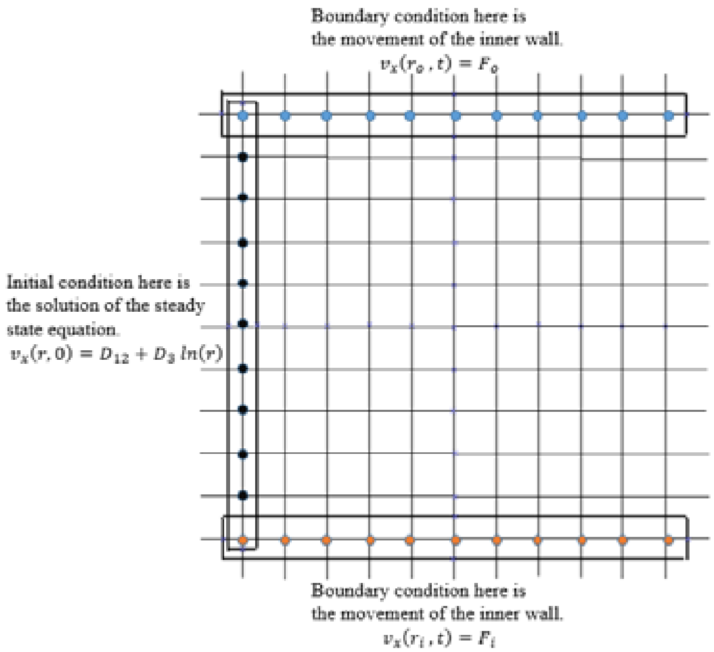

Fig. 2. Specifying initial and boundary conditions

Figure (2) shows the discretization of the annular and the known initial boundary values of grid points. Using boundary conditions values are obtained at the grids of the inner wall and outer wall and the initial condition values are used for $t = 0$. Hence, subsequent values are approximated

3. RESULTS AND DISCUSSION

Finite difference method was programmed in MATLAB to visualize the suddenly stopped axial Couette flow for various cases between the inner pipe and outer pipe in (annular space).

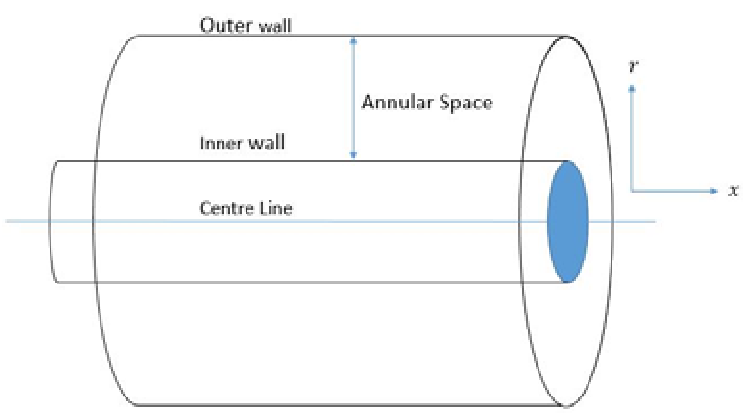

Fig. 3. Schematic description of annular space in axial direction.

3.1 Case I

In this case the outer pipe was fixed and the inner pipe was moving at a constant velocity in axial direction and the inner pipe was suddenly stopped.
Figure (3) shows the streamlines at different radii ratios (η), 0.1, 0.3, 0.5 and 0.7 when initially the inner pipe was moving and suddenly the inner pipe was brought to rest. With respect to the radius ratios there is a significant change in streamlines of the flow field.

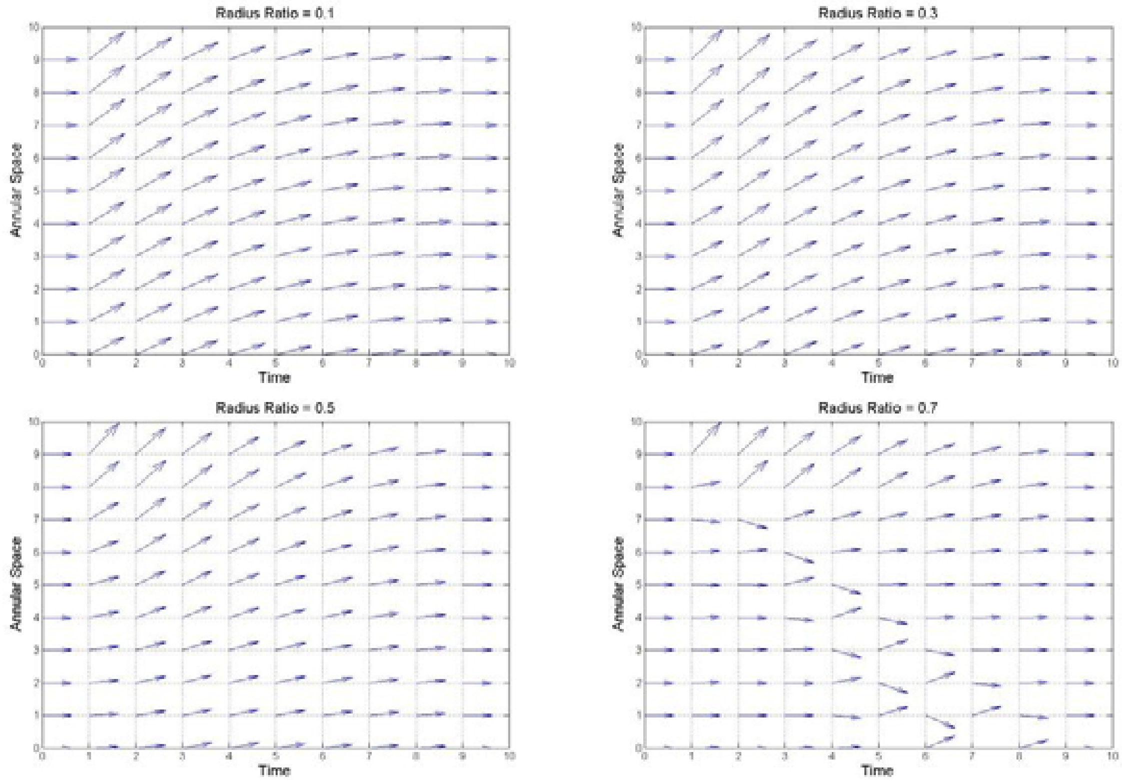

Fig. 4. Streamline for suddenly stopped axial Couette flow at different radius ratios for Case I when inner pipe moving at a constant velocity and outer pipe at rest (Time and annular space are non-dimensional)

Figure (4) shows the points of discrete values of velocity profile at different time steps. Due to the viscosity of the fluid, near to inner boundary velocity was maximum and at the outer boundary the velocity was zero. Initially inner pipe was moving at a constant velocity and outer pipe was at rest. Then, the inner pipe was brought to rest suddenly. There was a decay in velocity profile was observed with respect to time.

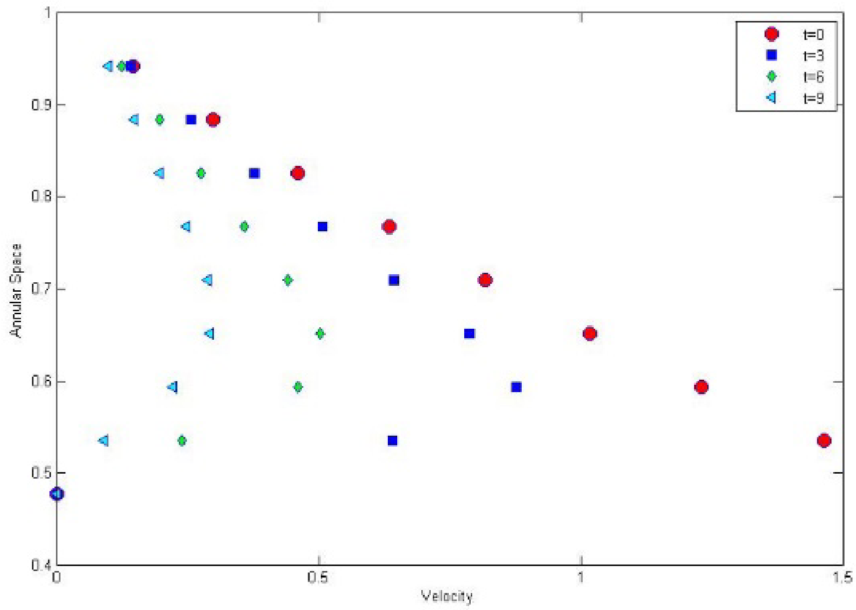

Fig. 5. Velocity profiles at different times for Case I when initially inner pipe moving at a constant velocity and outer pipe at rest at $\eta = 0.477$ (Velocity and annular space are non-dimensional)

3.2 Case II

When inner pipe and outer pipe were moving at a constant velocity and both pipes were suddenly stopped.
For the different radius ratios (η), 0.1, 0.3, 0.5 and 0.7, streamlines of the suddenly stopped Couette flow is obtained when initially inner pipe and outer pipe is moving at a constant velocity. Figure (5) shows the flow field at different radius ratios. With respect to the radius ratios notable difference in the streamlines of the flow field is noticed.

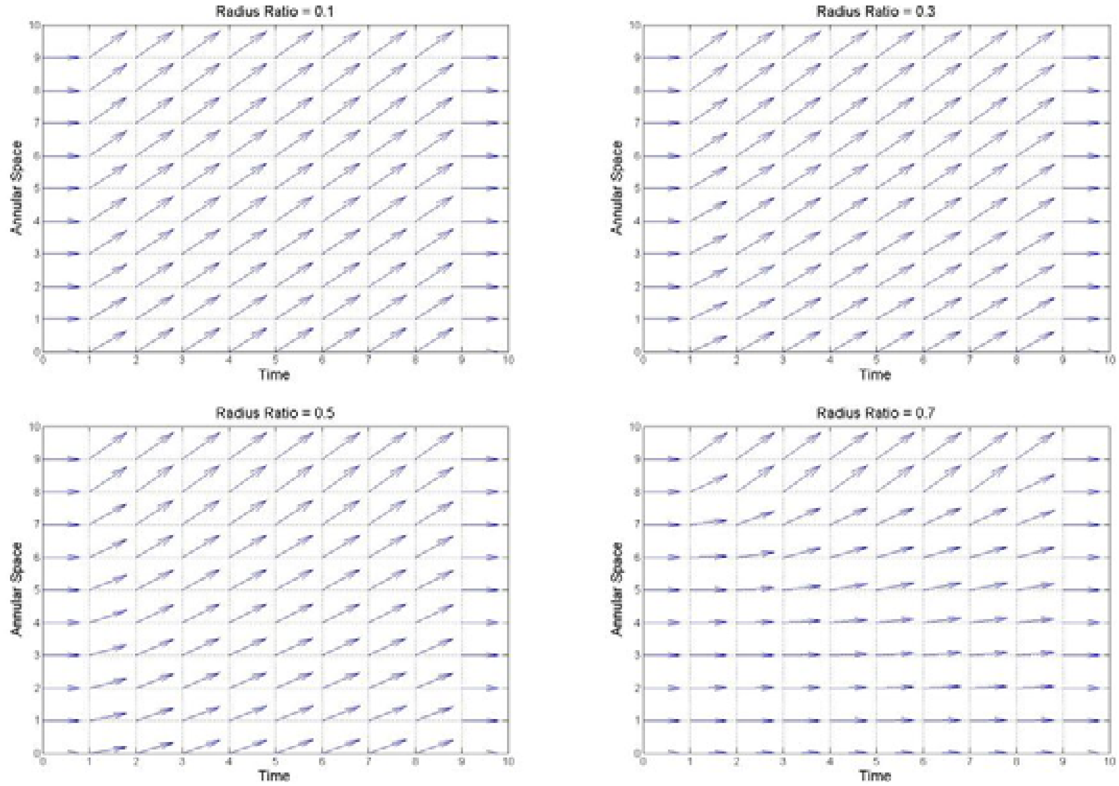

Fig. 6. Streamline for suddenly stopped axial Couette flow at different radius ratios for Case II when initially inner and outer pipes moving at same constant velocity (Time and annular space are non-dimensional)

Figure (6) represents the points of discrete values of velocity profile at different time steps. In this case inner and outer boundaries are moving at a constant velocity. Boundaries are moving with the same velocity and asymmetry in the velocity profiles are observed.

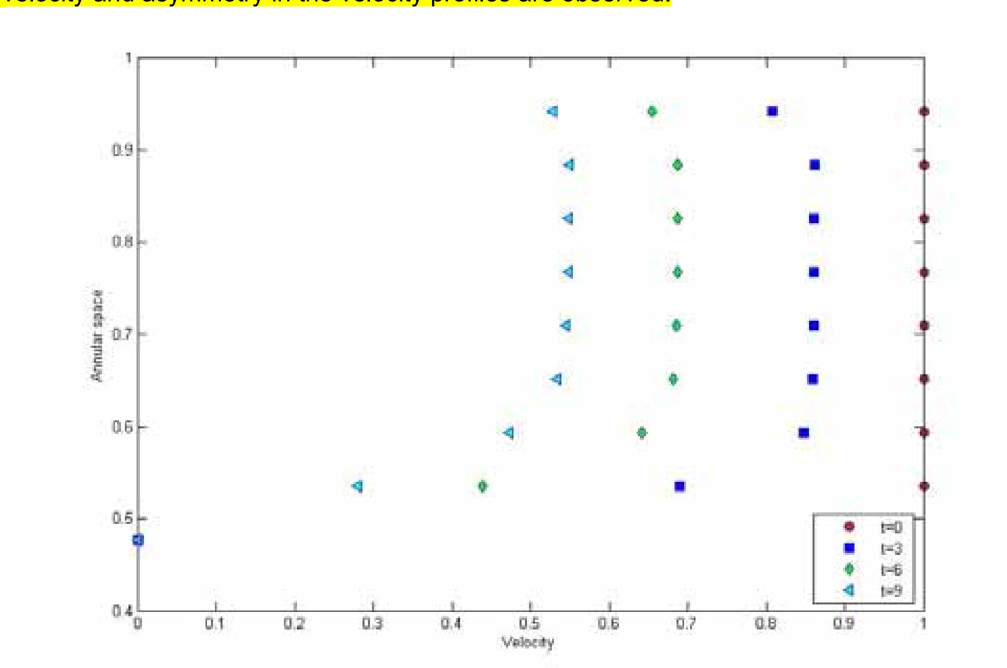

Fig. 7. Velocity profiles at different times for Case II when initially inner and outer pipes moving at same constant velocity at $\eta = 0.477$ (Velocity and annular space are non-dimensional)

3.3 Case III

When inner pipe and outer pipe initially moving at different velocities (V_i and V_o) and both pipes are stopped suddenly.

Figure (7) denotes the streamlines of the abruptly stopped axial Couette flow when inner boundary and outer boundary have different constant velocities. In the flow field the change in streamlines are significant.

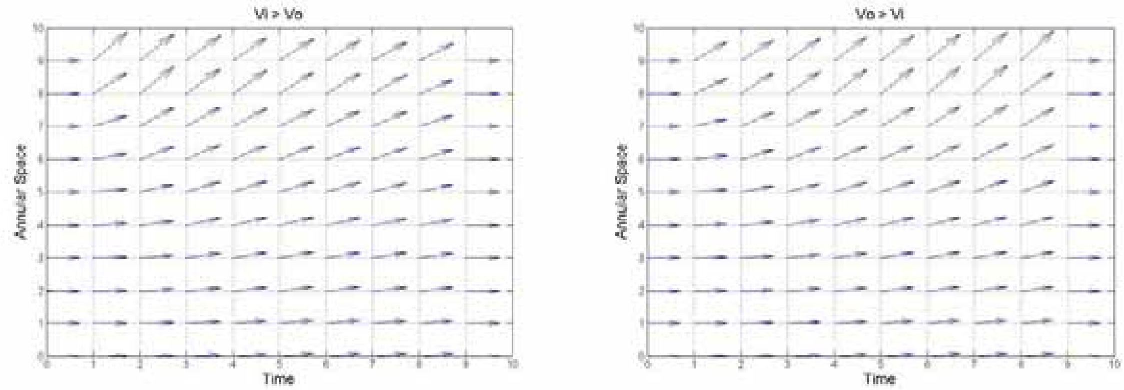

Fig. 8. Streamline of suddenly stopped axial Couette flow for Case III when inner and outer pipes in different constant velocities (Time and annular space are non-dimensional)

Figure (8) shows the points of discrete values of velocity profile at different time steps when initially inner boundary moving faster than outer boundary and both are brought to rest suddenly.

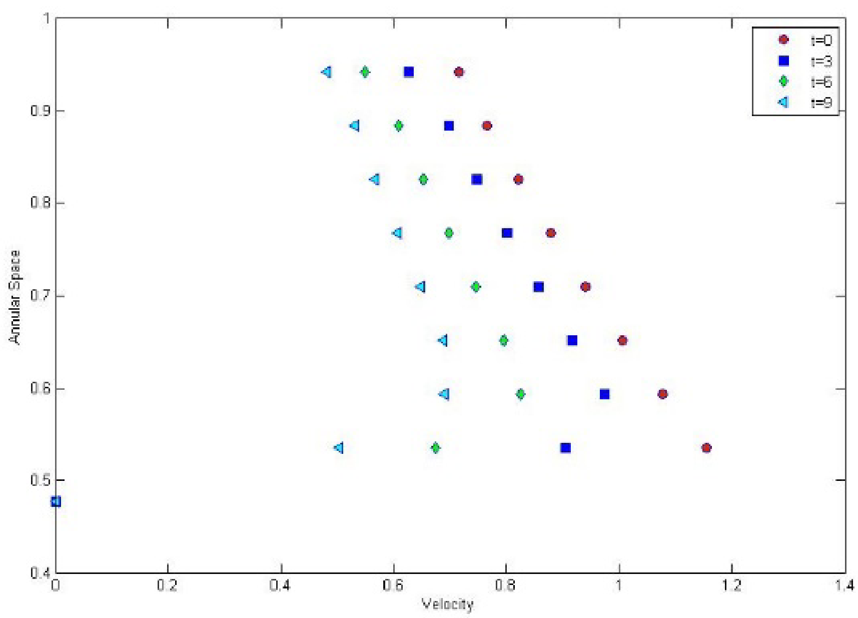

Fig. 9. Velocity profiles for abruptly stopped pipes at different times for Case III when $V_i > V_o$ at $\eta = 0.477$ (Velocity and annular space are non-dimensional)

Figure (9) represents the points of discrete values of velocity profile at different time steps when initially outer boundary moving faster than inner boundary and both are suddenly stopped.

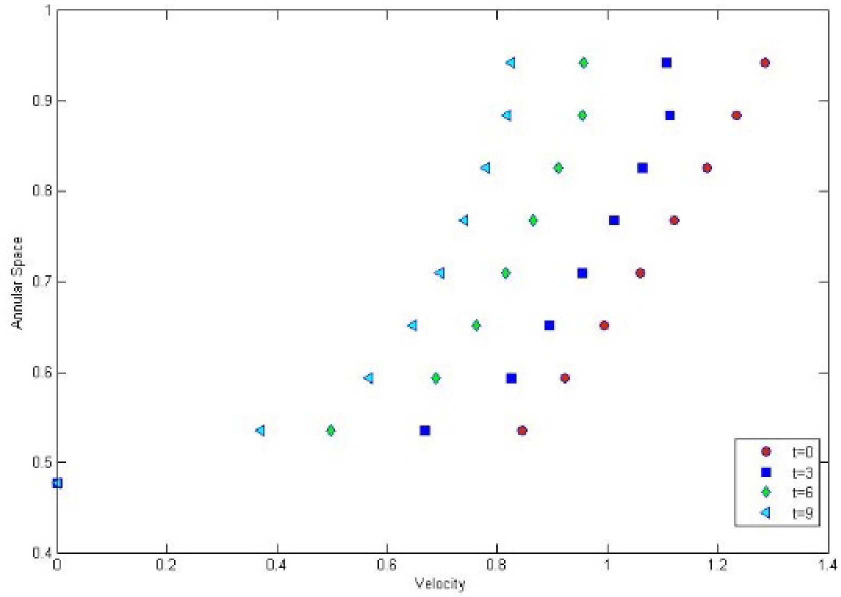

Fig. 10. Velocity profiles for abruptly stopped pipes at different times for Case III when $V_o > V_i$ at $\eta = 0.477$ (Velocity and annular space are non-dimensional)

4. CONCLUSION

In the work presented, the second order non-homogeneous partial differential equation was solved to obtain the solution for Couette flow. The numerical approximation for the unsteady abruptly stopped axial Couette flow was modelled using FDM. Three different cases were analysed in MATLAB programming, to visualize the flow field and streamline and velocity profiles at different time steps were obtained.

In case I, initially the inner boundary was moving at a constant velocity and it was suddenly stopped. Streamlines for various radius ratios (η), 0.1, 0.3, 0.5 and 0.7 were obtained in Figure (3). In case II, initially inner and outer boundaries were moving at same constant velocity and both boundaries were suddenly stopped. Streamlines for various radius ratios (η), 0.1, 0.3, 0.5 and 0.7 were obtained in figure (5). In both cases significant differences in streamlines of the flow field were visualized. In case III, initially inner boundary and outer boundary had different velocities. Streamlines were visualized in figure (7).

Different cases play different role in the flow characteristics of the annular flow. Flow characteristics were changed due to the asymmetry of velocity profiles and unsteadiness of flow field. The asymmetry of the velocity profile was affected by different radius ratios. Unsteadiness in the flow field was happened due to sudden changes in flow parameters. So, these sudden changes in the flow parameter and different radius ratios play important roles in the stability of the flow.

This work presents the analytical and numerical solution and the approach for the solution for abruptly stopped axial Couette flow. The stability analysis can be carried out to analyse the stability of the flow when a small disturbance is introduced to the flow. Which may help to understand and predict the instability. The non-linear stability analysis could help in understanding the transition to turbulent process which is not addressed in this work. We plan to use MATCONT continuation software to perform a non-linear stability analysis [17]. Non-concentric annulus with bidirectional flow may give the solution for the real world applications with minimizing assumptions.

REFERENCES

[1] R. W. Hanks and J. M. Peterson, "Complex transitional flows in concentric annuli," AIChE J., vol. 28, no. 5, pp. 800–806, Sep. 1982.

[2] Y. Wang and G. A. Chukwu, "Unsteady Axial Laminar Couette Flow of Power-Law Fluids in a Concentric Annulus," Ind. Eng. Chem. Res., vol. 35, no. 6, pp. 2039–2047, Jan. 1996.

[3] E. P. F. de Pina and M. S. Carvalho, "Three-Dimensional Flow of a Newtonian Liquid Through

an Annular Space with Axially Varying Eccentricity," J. Fluids Eng., vol. 128, no. 2, p. 223, 2006.
[4] D. Das and J. H. Arakeri, "Transition of unsteady velocity profiles with reverse flow," J. Fluid Mech., vol. 374, pp. 251–283, 1998.
[5] D. DAS and J. H. Arakeri, "Unsteady Laminar Duct Flow With a Given Volume Flow Rate Variation," J. Appl. Mech., vol. 67, no. June 2000, pp. 274–281, 2000.
[6] M. E. Erdoğan, "On the flows produced by sudden application of a constant pressure gradient or by impulsive motion of a boundary," Int. J. Non. Linear. Mech., vol. 38, no. 5, pp. 781–797, 2003.
[7] A.-S. Yang and T.-C. Kuo, Blowdown and fluid hammer studies for a satellite reaction control subsystem, vol. 215. 2001.
[8] A. Nayak, "On one dimensional unsteady flow through pipe and annular region between two concentric pipes for a given volume flow rate variation: Exact solution and three dimensional linear stability analysis," IIT, Kanpur, 2005.
[9] M. Dibakar, "Exact solution and linear stability analysis of unsteady sliding Couette-Poiseuille flow," IIT, Kanpur, 2012.
[10] K. Ashok, "Instability of unsteady annular pipe flow: Theoretical and experimental investigation," IIT, Kanpur, 2012.
[11] H. M. I. U. Herath, J. A. Weliwita, S. M. V. P. D. Senanayake and S. Witharana, "Effect of moisture content on cooking time of rice," 2016 Manufacturing & Industrial Engineering Symposium (MIES), Colombo, 2016, pp. 1-5. doi: 10.1109/MIES.2016.7780257
[12] F. M. White, "Viscous Fluid Flow Viscous," New York, vol. Second, p. 413, 2000.
[13] J. Harrison, "Fast and Accurate Bessel Function Computation," in 2009 19th IEEE Symposium on Computer Arithmetic, 2009, pp. 104–113.
[14] W. G.A, A treatise on the theory of Bessel functions., 2nd ed. Cambridge University Press, 1944.
[15] C. M. Bender and S. A. Orszag, Advanced Mathematical Methods for Scientists and Engineers I. New York, NY: Springer New York, 1999.
[16] M. Spiegel, Schaum's Outline of Laplace Transforms. McGraw-Hill, 1965.
[17] J. A. Weliwita, "Spiral Defect Chaos and the Skew-Varicose Instability in Generalizations of the Swift-Hohenberg Equation," University of Leeds, 2011.